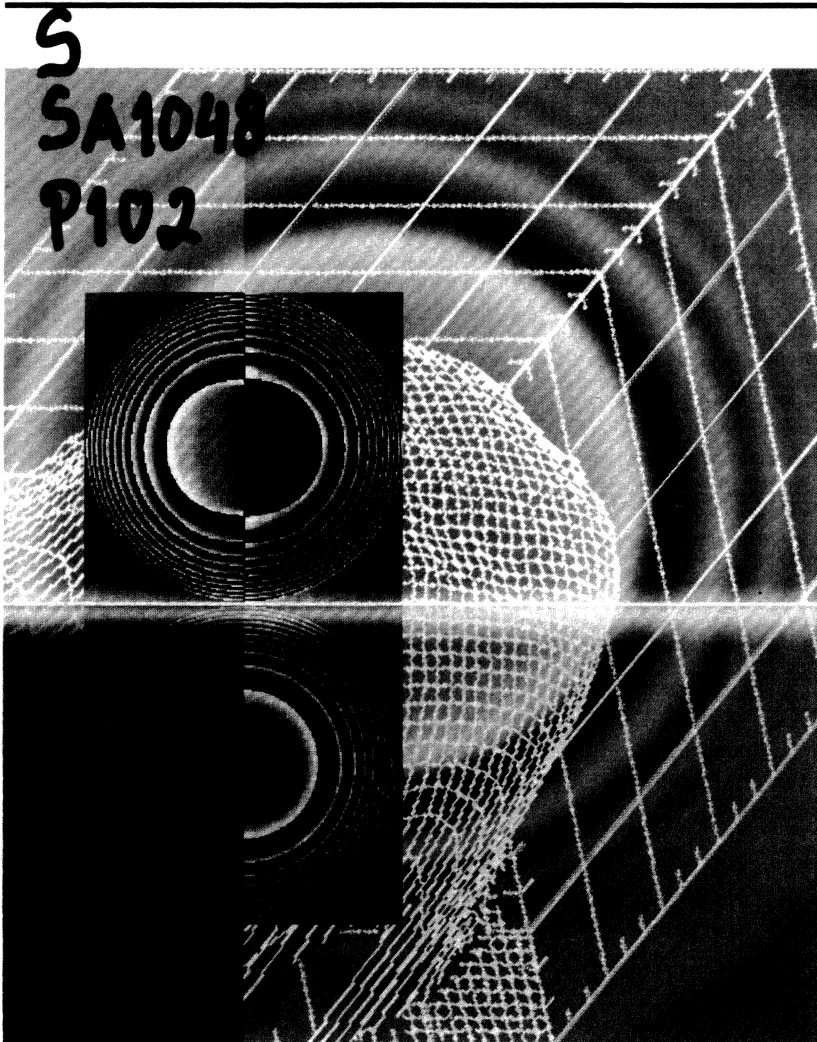


December 2003
Volume 42 Number 12
ISSN 0091-3286

OPTICAL ENGINEERING

SPIE—
The International
Society for
Optical Engineering



- OE Letters
 - Acousto-Optical Tunable Filters
 - Diffractive Optics
 - Optical Clock Generation
 - Optical Logic Generation
 - Optical Switches
 - Waveguide Gratings
 - Wavelength Monitors
- Featuring Papers on
 - Automated Visual Inspection
 - Crack Measurement
 - Digital Holography
 - Fiber Amplifiers
 - Fiber Bragg Gratings
 - Fiber Dispersion
 - Image Reconstruction
 - Image Restoration
 - Infrared Beamsplitters
 - Infrared Detectors
 - Infrared-to-Visible Converters
 - Interferometry
 - Laser Heat Treating
 - Liquid Crystals on Silicon
 - Motion Blur
 - Optical Encryption
 - Optical Sensors
 - PLZT Thin Films
 - Polarizers
 - Position Estimation
 - Profilometry
 - Radiometric Calibration
 - Time-of-Flight Range Finders
 - Ultraviolet Lasers
 - X-Ray Optics

This resource is also available
on the WWW.
Use MadCat to launch.

**DOCKET
ALARM**

Find authenticated court documents without watermarks at docketalarm.com.

OPTICAL ENGINEERING

Donald C. O'Shea
Editor

Editor

Donald C. O'Shea
Georgia Institute of Technology
School of Physics
Atlanta, Georgia 30332-0430
404/894-3992 • Fax 404/894-9958
E-mail doshea@prism.gatech.edu

Editorial Board

James Bilbro
NASA Marshall Space Flight Ctr.
Optical fabrication & testing, coherent lidar

Luc R. Bissonnette
Defence Research Establishment Valcartier
Lidar, aerosol scattering

Casimer DeCusatis
IBM Corporation
Fiber optics

Ronald G. Driggers
Army Research Lab.
Infrared systems and radiometry

Touradj Ebrahimi
Swiss Federal Institute of Technology EPFL
Image/video processing and coding

G. Groot Gregory
Lambda Research Corp.
Interferometry

Jürgen Jahns
University of Hagen, Germany
Optical interconnects, micro-optics

François Kajzar
CEA Saclay
Nonlinear optics

Ali Khounsary
Argonne National Lab.
X-ray optics, high-heat-load optics

Raymond K. Kostuk
University of Arizona
Holographic materials, processes, and systems

H. Angus Macleod
Thin Film Center
Thin film technology

Dennis W. Prather
University of Delaware
Physical optics

Gregory J. Quarles
VLOC
Lasers

Jennifer C. Ricklin
Army Research Laboratory
Atmospheric optics

Giancarlo C. Righini
IROE, National Research Council
Integrated optics

Jannick P. Rolland
School of Optics and CREOL at UCF
Optical system design

Rajpal S. Sirohi
Indian Inst. of Technology Madras
Interferometry

Bryan D. Stone
Optical Research Associates
Lens design

Andrew G. Tescher
Compression Science Corporation, Inc.
Image compression, image & signal processing, video technologies

Tomasz R. Wolinski
Warsaw University of Technology
Optical fiber sensors and liquid crystals

Jiangying Zhou
Summus Ltd.
Image analysis, pattern recognition and computer vision

Managing Editor

Karolyn Labes
P. O. Box 10
Bellingham, Washington 98227-0010
360/676-3290 • Fax 360/647-1445
E-mail journals@spie.org

Editorial Staff

Monica Crabtree
Rita J. Davis
Michelle Luff
Anne Munger

Publisher

Eugene G. Arthurs, *Executive Director*
Eric Pepper, *Director of Publications*

Mailing:
SPIE
P.O. Box 10
Bellingham, Washington 98227-0010

Shipping:
SPIE
1000 20th Street
Bellingham, Washington 98225
360/676-3290 • Fax 360/647-1445
E-mail journals@spie.org

Copyright © 2003, The Society of Photo-Optical Instrumentation Engineers. Copying of material in this journal for internal or personal use, or the internal or personal use of specific clients, beyond the fair use provisions granted by the U.S. Copyright Law is authorized by SPIE subject to payment of copying fees. The Transactional Reporting Service base fee for this journal is \$15.00 per article (or portion thereof), which should be paid directly to the Copyright Clearance Center (CCC), 222 Rosewood Drive, Danvers, MA 01923. Other copying for republication, resale, advertising or promotion, or any form of systematic or multiple reproduction of any material in this journal is prohibited except with permission in writing from the publisher. The CCC fee code for this journal is 0091-3286/03/\$15.00.

Editorial. Send manuscripts and technical correspondence to SPIE. Papers and reviews published in *Optical Engineering* reflect the opinion of the author(s); inclusion of articles and advertisements does not necessarily constitute endorsement by the editors or by SPIE.

SPIE Membership. Annual membership dues include a choice of the Society's four peer-reviewed journals. 2003 membership dues: \$95; \$45 Retired; \$40 Student. For more information, contact SPIE Membership Services at 360/676-3290, Fax 360/647-1445, e-mail: membership@spie.org. **Change of Address.** Send old and new address to SPIE Headquarters.

Optical Engineering (ISSN 0091-3286) (USPS 450-970) is published monthly by the Society of Photo-Optical Instrumentation Engineers, 1000 20th St., Bellingham, WA 98225 at the following annual subscription prices: print plus online, \$550 N. America, \$615 outside N. America. Periodicals postage paid at Bellingham, WA 98225, and at additional mailing offices. **Postmaster:** Send address changes to *Optical Engineering*, 1000 20th St., Bellingham, WA 98225.

Printed in the United States on acid-free paper.

Contributions for optics education. SPIE, a non-profit public benefit corporation, gratefully accepts tax-deductible contributions and bequests in support of its efforts to foster interaction and to advance knowledge in optical and optoelectronic applied science and engineering. With special emphasis on education, SPIE annually awards scholarships and publishes a guide to optics programs in colleges and universities around the world. The Society has established a fund to support student travel to SPIE symposia and is facilitating donations of technical publications to educational institutions and libraries without access to this literature. For information on how you can contribute or participate in a deferred-giving program, please contact Sharon Kirkpatrick, SPIE Headquarters, P.O. Box 10, Bellingham, WA 98227-0010, 360/676-3290, Fax 360/647-1445, E-mail sharonk@spie.org.

Optical pumping of the XeF(C→A) and iodine 1.315- μm lasers by a compact surface discharge system

B. A. Knecht*

R. D. Fraser†

D. J. Wheeler‡

C. J. Zietkiewicz§

A. A. Senin, MEMBER SPIE

L. D. Mikheev||

V. S. Zuev||

J. G. Eden

University of Illinois

Department of Electrical and Computer
Engineering

Laboratory for Optical Physics and
Engineering

Urbana, Illinois 61801

Abstract. Details are provided regarding the design, construction, and performance of a compact ($\approx 0.6\text{-m}^2$ footprint), single-channel surface discharge system and its application to optically pumping the XeF(C→A) and iodine atomic lasers in the blue-green ($\approx 480\text{ nm}$) and near infrared ($1.315\ \mu\text{m}$), respectively. The system has a gain (active) length of $\approx 50\text{ cm}$, and triggering the discharge requires no high-voltage or high-current switches. Measurements of the velocity of the photodissociation bleaching wave and the small-signal gain of the XeF(C→A) system are described. At 488 nm , the gain coefficient γ was found to be $\approx 0.3\% \text{ cm}^{-1}$, a value comparable to those reported previously for systems dissipating considerably higher power per unit length. Single-pulse energies $> 50\text{ mJ}$ from the XeF(C→A) laser ($\approx 485\text{ nm}$) and $> 0.7\text{ J}$ on the $5p^2P_{1/2} \rightarrow 5p^2P_{3/2}$ transition of atomic iodine at $1.315\ \mu\text{m}$ have been obtained with nonoptimized resonator output couplings (5% and 10%, respectively). The rate of erosion of the dielectric surface has been measured to be ≈ 0.1 to $0.3\ \mu\text{m}/\text{shot}$ for a glass ceramic dielectric, and the performance of two electrical configurations for the ballasting pins (feedthrough and V) is compared. © 2003 Society of Photo-Optical Instrumentation Engineers. [DOI: 10.1117/1.1624849]

Subject terms: lasers; visible; optical pumping; surface discharge.

Paper 030139 received Mar. 24, 2003; revised manuscript received Jun. 9, 2003; accepted for publication Jun. 10, 2003.

1 Introduction

The surface discharge, an electric discharge at the interface of a gas and a solid dielectric, was first reported by G. C. Lichtenberg in 1777. Over the past three decades, renewed interest in surface discharges has been driven by potential applications in materials processing,¹ surface cleaning,^{2,3} waste remediation, and optical pumping of lasers by photodissociation,⁴⁻⁶ all of which require intense sources of ultraviolet (UV) or vacuum ultraviolet (VUV) radiation.

Excitation of lasers by a surface discharge is particularly attractive because of the ability of the optical source to produce quasi-blackbody radiation having a characteristic temperature above $3 \times 10^4\text{ K}$ and to do so with a relatively simple system amenable to repetitively pulsed operation. In 1975, Beverly⁵ proposed pumping the iodine photodissociation laser ($5p^2P_{1/2} \rightarrow 5p^2P_{3/2}$; $\lambda = 1.315\ \mu\text{m}$) with a surface discharge and subsequently measured efficiencies approaching 10% and 3% for the conversion of electrical

power to optical radiation in the 250- to 290-nm and 170- to 210-nm spectral regions, respectively.⁷ Studies have also shown surface discharges to be effective sources of extreme ultraviolet (XUV; $\hbar\omega \approx 10$ to 70 eV) photons,³ and characteristic radiation temperatures of $(1$ to $2) \times 10^4\text{ K}$ are attainable for specific energy loadings of the plasma of 1 to 4 J cm^{-2} (Ref. 5). In 1979, Belotserkovets et al.⁸ demonstrated lasing from atomic iodine when the molecular precursor, $\text{C}_3\text{F}_7\text{I}$, was photolyzed by a surface discharge. Since that time, a variety of atomic and molecular lasers initiated or pumped entirely by a surface discharge have been demonstrated,^{4,9} but much of the effort has been directed toward the XeF photodissociation laser,^{10,11} partly because of the breadth of the absorption spectrum of the parent molecule, XeF_2 . The other factors providing impetus for the efforts on XeF are the two laser transitions that are available (B→X and C→A) as well as the large saturation intensity of the C→A band in particular.¹² The latter, $\approx 400\text{ kW cm}^{-2}$, is a direct reflection of both the C-A stimulated emission cross section ($\approx 9 \times 10^{-18}\text{ cm}^2$) and the C-state radiative lifetime ($93 \pm 5\text{ ns}$).¹³

In a series of papers published between 1984 and the early 1990s (Refs. 14 to 17), Kashnikov, Zuev and co-workers reported the characteristics of a sequence of surface-discharge-pumped XeF laser systems producing as much as 174 J on the B→X transition of the molecule in

*Present address: 662N 300W, Lebanon, IN 46052.

†Present address: Realized Technologies Inc., 1530 Barclay Blvd., Buffalo Grove, IL 60089.

‡Present address: National Center for Supercomputing Applications (NCSA), University of Illinois, 605 E. Springfield, Champaign, IL 61820.

§Present address: Melles Griot, 2605 Trade Center Avenue, Longmont, CO 80503.

||Permanent address: P. N. Lebedev Physical Institute, Moscow, Russian Federation

the UV at 351 nm and up to 117 J in the blue-green ($C \rightarrow A$ transition, $\lambda \approx 485$ nm). Consisting of individual discharge sections, each typically 8 to 12 cm in length and having a dedicated capacitor and high-voltage switch, these optical sources had active lengths ranging from 70 to 190 cm. The first system, reported by Kashnikov et al.,¹⁴ comprised eight discharge sections in a single-channel design and yielded a brightness temperature of $\approx 3 \times 10^4$ K. By increasing the gain length to 190 cm (16 discharge sections), raising the number of discharge channels to three, and with careful attention given to the current rise time and the purity of the XeF₂ vapor, the Russian group subsequently produced single-pulse energies that are, to this day, unsurpassed for a primary coherent source in the visible.¹⁷

Despite the impressive characteristics of these lasers, including the ability to operate at a pulse repetition frequency of 1 Hz, the system was quite large, and the dedication of a capacitor and high current switch to each discharge section introduced significant timing jitter ($< 0.25 \mu\text{s}$). Furthermore, in low-impedance circuits of this type, switches consume substantial energies and adversely affect the complexity and lifetime of the system.

In the mid-1990s, we reported the design and preliminary operation of a compact surface discharge system that successfully pumped the XeF($C \rightarrow A$) and iodine photodissociation lasers.^{18,19} A more detailed account of the design and operation of this system and an alternative structure for the surface discharge ignition electrodes are presented here. Having an active length of ≈ 50 cm, this surface discharge system requires no high-voltage (or high-current) switches, which has the beneficial result of lowering the firing jitter as well as the equivalent series inductance for the system. Careful attention given to the design and layout of the device and the power generator has resulted in a rugged system having a compact footprint ($\approx 0.6 \text{ m}^2$) and an overall size comparable to that of a commercial excimer laser. The small-signal gain on the $C \rightarrow A$ transition of XeF has been measured to be $0.3\% \text{ cm}^{-1}$ at 488 nm, a value virtually identical to those reported for surface discharge systems of considerably higher power loadings.

This paper is organized as follows. Section 2 describes in detail the design of the electrical system and laser head for the device. Two approaches to igniting the surface discharge, surface feedthrough (in-line) and V configurations, are presented and compared. The experimental results on the XeF($C \rightarrow A$), XeF($B \rightarrow X$), and atomic iodine (1.315 μm) lasers are discussed in Sec. 3, and Sec. 4 summarizes the conclusions of this study.

2 Surface Discharge System: Design and Performance

2.1 Background

Previous designs of surface discharge systems can be broadly classified into two groups. The first are those in which the discharge occurs on a dielectric surface such as polyethylene, Teflon, or a ceramic^{9,14-17} and the distance d between consecutive electrodes ranges from several centimeters to beyond 10 cm. The practical upper limit on the discharge gap is dictated by the breakdown voltage for a

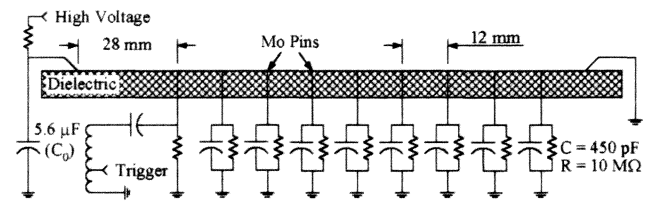


Fig. 1 Schematic diagram of the feedthrough (in-line) electrical configuration for igniting and sustaining a surface discharge. The Mo pins are ballasted capacitively and resistively, and the charging voltage is typically 30 kV. The dielectric surfaces explored to date are machinable glass ceramic, BN, and Al₂O₃ and SiC-coated surfaces.

which rises dramatically with increasing d . If no accommodations are made for triggering the discharge or preionizing the gap, charging voltages of ≥ 15 –30 kV are required, even for small gaps ($d \approx 2$ –3 cm), to obtain an adequate radiation temperature. Systems with long gain lengths, such as the devices of Refs. 14–17, having active lengths of 0.7–1.9 m, rely on discharge sections operated in tandem. Each section, typically 8–12 cm in length, requires 10 kV when the entire discharge is triggered by a 50-kV pulse applied to a cable lying beneath the dielectric surface. The device of Ref. 16, for example, had a gain length of 1.9 m as a result of 16 individual discharge sections, each 12 cm in length.

The second general category of devices relies on discharges produced on the surface of ferrite rods or slabs. Producing a stable, intense surface discharge with these materials requires forming a channel in the ferrite, either by exploding a wire on its surface²⁰ or by micromachining a narrow channel ($\approx 150 \mu\text{m}$) by laser ablation.²¹ Such devices typically involve rods tens of centimeters in length (76 cm in Ref. 20) and driven by a capacitor charged to 40 to 50 kV. To summarize, realizing in a surface discharge system the gain lengths normally required for high-power laser operation (tens of centimeters) requires a means for spatially confining the discharge. Long path lengths can be obtained with ferrites once a channel has been established on the surface, or shorter discharge sections (≈ 10 cm) can be combined in tandem to yield active lengths beyond 1 m.²⁰⁻²⁴

2.2 Electrical Design: Power Generator and Discharge Ignition Configurations

The approach adopted for the experiments reported here offers a novel and robust scheme for establishing surface discharges over paths of arbitrary length and to do so without the need to switch each section independently. In fact, no high-current or high-voltage switches are used at all. Rather, the discharge functions as its own switch.

A schematic diagram of the first electrode configuration investigated is shown in Fig. 1. The key elements of this surface discharge device are: a ceramic substrate that runs parallel to the discharge axis, a main electrode at each end, and a series of intermediate electrodes between the main electrodes which divide the discharge path into segments. The critical feature of this design is the latter—a series of resistively and capacitively-ballasted molybdenum pins,

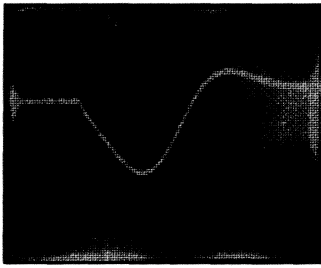


Fig. 2 Oscilloscope trace of the surface discharge current for a charging voltage of ≈ 30 kV. The horizontal (temporal) scale is $2 \mu\text{s}/\text{div}$, and the vertical scale is $20 \text{ kA}/\text{div}$.

charge. All of the pins in the linear array were isolated from dc ground by a $10\text{-M}\Omega$ resistor and a 450-pF doorknob capacitor. For the first pin (trigger electrode), however, the capacitor was connected in series with the secondary of an air-core autotransformer, to which the trigger pulse was applied. The separation between the pins in the array, except that between the high-voltage (HV) and trigger electrodes was set at 12.7 mm ($1/2 \text{ in.}$) to ensure that breakdown between two adjacent pins occurred at or below 30 kV when the gas pressure in the laser chamber was 1 atm . The gap between the HV electrode (left side, Fig. 1) and the trigger electrode was set to 28 mm (designed to hold off 30 kV). Consequently, when the full supply voltage was impressed across the entire array (HV electrode to ground), breakdown does not occur in the absence of a trigger pulse. However, when a -15 to -18-kV trigger pulse is applied to the transformer primary, the voltage appearing on the first pin (trigger electrode) is -50 kV , and breakdown occurs in the HV-electrode-trigger-electrode gap. As current begins to flow in this gap, the voltage at the trigger electrode rises rapidly to a value slightly above 30 kV , owing to peaking effects. Since the second pin in the array is still at ground potential, the gap between the trigger electrode (pin 1) and pin 2 now self-breaks. The remaining gaps in the array follow in quick succession, and within $5 \mu\text{s}$ of the application of the trigger pulse, a surface discharge is established along the entire length of the array. A major advantage of this design is that the individual gaps are not triggered independently and, consequently, the firing jitter (with respect to the command trigger) is low. Furthermore, although negative trigger pulses were normally employed in the experiments described here, the use of an autotransformer reduces the sensitivity of the system to the polarity of the trigger (because of ringing in the secondary of the transformer), resulting in improved reliability and stability.

Little of the energy stored in the capacitor bank ($5.6 \mu\text{F}$ cf. Fig. 1) is expended in forming the discharge, but the establishment of the surface discharge presents a low-impedance path to ground. It is at this point that C_0 delivers virtually all of its stored energy to the discharge, resulting in rapid heating of the plasma and the generation of intense blackbody radiation. It should be mentioned that once the discharge is established, negligible current flows through the ballasting pins, which are effectively decoupled from ground.

Figure 2 is an oscilloscope trace of the discharge current, obtained with 1 atm of air in the laser head and a machinable glass ceramic (MACOR) serving as the dielectric. The



Fig. 3 Photograph of the surface discharge. The path length is 48.5 cm .

waveform, recorded by a modified Rogowski coil for a charging voltage on the capacitor bank of 30 kV , is representative of those observed throughout these experiments and shows that the current reaches its peak value of $\approx 46 \text{ kA}$ in $\approx 4 \mu\text{s}$. The maximum current observed to date is $>50 \text{ kA}$. Notice that the current waveform is essentially critically damped, indicating that the impedance of the capacitor bank nearly matches that of the surface discharge. This is a result of efforts from the earliest designs to minimize the inductance of the power generator and laser head. Consequently, $>80\%$ of the 2.5 kJ stored in the capacitor bank (for $V = 30 \text{ kV}$) is deposited in the surface discharge in the first half cycle of the current waveform. For a power pulse having a temporal width of $5 \mu\text{s}$ (FWHM), this energy dissipation corresponds to a power deposition per unit length of discharge of $\approx 8 \text{ MW cm}^{-1}$.

The low overall inductance of the capacitor bank and electrical connections to the HV and ground electrodes manifested itself in an unusual way during the testing of this system. Early versions of the laser employed standard wire to connect the ballast circuitry to the intermediate electrodes. To facilitate the rapid assembly of the laser head, the wire was later replaced by short springs, but experience showed that it was necessary to carefully limit the number of turns in the coils. Otherwise, the inductive voltage drop produced across the spring resulted in arcing and severe damage to the coil and associated components.

Although the primary purpose of the Mo pins is to enable the rapid formation of a surface discharge over a path of arbitrary length with a moderate voltage, the pin array also serves to confine the discharge, thereby improving the shot-to-shot reproducibility with respect to previous surface discharge devices. Figure 3 is a photograph of the surface discharge viewed normal to the surface. Minor deviations from a straight path are evident, and the overall length of the surface discharge is 48.5 cm .

2.3 Laser Head: In-Line and V Configurations

Side, frontal, and end-on views of the laser head with the in-line ballast pin array configuration described in the last section are illustrated schematically in Fig. 4. Each Mo pin was inserted into a cylindrical hole in the dielectric material and was mounted so that its tip was flush with the surface of the dielectric. For most of the experiments reported here, MACOR machinable ceramic served as the dielectric material, but preliminary tests with pyrolytic boron nitride, alumina, and SiC-coated surfaces were also conducted. Because of its chemical stability in the presence of fluorine, Kynar® was the material from which the laser head was machined. The lower plate (not shown in Fig. 4) sealing the laser head was fabricated from a polycarbonate or aluminum. As noted earlier, both the main electrodes and the intermediate (pin) electrodes enter the laser head through the top and traverse the ceramic dielectric. The seal around the main electrodes consisted of a Kynar fitting having a

Explore Litigation Insights

Docket Alarm provides insights to develop a more informed litigation strategy and the peace of mind of knowing you're on top of things.

Real-Time Litigation Alerts



Keep your litigation team up-to-date with **real-time alerts** and advanced team management tools built for the enterprise, all while greatly reducing PACER spend.

Our comprehensive service means we can handle Federal, State, and Administrative courts across the country.

Advanced Docket Research



With over 230 million records, Docket Alarm's cloud-native docket research platform finds what other services can't. Coverage includes Federal, State, plus PTAB, TTAB, ITC and NLRB decisions, all in one place.

Identify arguments that have been successful in the past with full text, pinpoint searching. Link to case law cited within any court document via Fastcase.

Analytics At Your Fingertips



Learn what happened the last time a particular judge, opposing counsel or company faced cases similar to yours.

Advanced out-of-the-box PTAB and TTAB analytics are always at your fingertips.

API

Docket Alarm offers a powerful API (application programming interface) to developers that want to integrate case filings into their apps.

LAW FIRMS

Build custom dashboards for your attorneys and clients with live data direct from the court.

Automate many repetitive legal tasks like conflict checks, document management, and marketing.

FINANCIAL INSTITUTIONS

Litigation and bankruptcy checks for companies and debtors.

E-DISCOVERY AND LEGAL VENDORS

Sync your system to PACER to automate legal marketing.